

# Does a distinct quasi many-body localized phase exist?

## A numerical study of a translationally invariant system in the thermodynamic limit

J. Sirker

*Department of Physics and Astronomy, University of Manitoba, Winnipeg R3T 2N2, Canada*

(Dated: January 1, 2019)

We consider a quench in an infinite spin ladder describing a system with two species of bosons in the limit of strong interactions. If the heavy bosonic species has infinite mass the model becomes a spin chain with quenched binary disorder which shows true Anderson localization (AL) or many-body localization (MBL). For finite hopping amplitude  $J'$  of the heavy particles, on the other hand, we find an exponential polarization decay with a relaxation rate which depends monotonically on  $J'$ . Furthermore, the entanglement entropy changes from a constant (AL) or logarithmic (MBL) scaling in time  $t$  for  $J' = 0$  to a sub-ballistic power-law,  $S_{\text{ent}} \sim t^\alpha$  with  $\alpha < 1$ , for finite  $J'$ . We do not find a distinct regime in time where the dynamics for  $J' \neq 0$  shows the characteristics of an MBL phase. Instead, we discover a time regime with distinct dephasing and entanglement times, leading to dynamics in this regime which is different *both* from a localized and from a fully ergodic phase.

### I. INTRODUCTION

The wave function of a single quantum particle in one dimension always becomes localized in a disorder potential.<sup>1–3</sup> Anderson localization (AL) of non-interacting quantum particles has been observed, for example, in ultracold gases.<sup>4,5</sup> Because AL is at its heart an interference phenomenon it has also been studied for classical waves.<sup>6</sup>

In recent years, the interplay of disorder and interactions in many-body quantum systems has attracted renewed interest.<sup>7</sup> Focussing on the one-dimensional case, a number of analytical and numerical studies have shown that, under certain conditions, a many-body localized (MBL) phase can occur breaking the ergodicity of the system.<sup>8–17</sup> A key signature of the fully many-body localized phase is the logarithmic spreading of entanglement entropy,  $S_{\text{ent}} \sim \ln t$ , under unitary time evolution starting from an unentangled initial state.<sup>18,19</sup> In contrast,  $S_{\text{ent}} \sim \text{const}$  at long times  $t$  in an AL phase. On the other hand, both in the AL and in the MBL phase the system retains memory of its initial state. This has been demonstrated in a cold gas experiment where an interacting quasi one-dimensional system was prepared in an initial charge-density wave state with the order parameter being stable over time.<sup>20</sup>

Another interesting question which has attracted attention recently but has been much less explored so far is whether translationally invariant many-body systems can also have *dynamically created* localized phases or at least extended time regimes where the dynamics appears to be localized ('quasi MBL') before thermalization ultimately sets in.<sup>21–27</sup> One of the defining properties of quasi-MBL according to Ref.26 where this terminology was introduced is that "The entanglement dynamics are consistent with MBL-type growth at short and intermediate times, but ultimately give way to anomalous diffusion." In contrast to disorder-induced MBL where localization occurs despite interactions, the idea here is that sufficiently strong interactions might actually induce true

localization or quasi MBL. Studies of spin chains with potential disorder in fact do provide evidence that very strong interactions can support localization. This can lead to a reentrant behavior where the system transitions at fixed disorder from Anderson  $\rightarrow$  MBL  $\rightarrow$  ergodic  $\rightarrow$  MBL with increasing interaction strengths.<sup>11,28,29</sup> On the other hand, translational invariance requires that for a finite-size system any finite wavelength inhomogeneity in the initial state decays to zero in the infinite time average (see Eq. (4) in Ref.26). True localization in a translationally invariant system therefore has to be understood as a divergence of the decay time for initial inhomogeneities with system size.<sup>26</sup> In the case of quasi MBL, on the other hand, the question is if an extended regime in time exists in which the decay of inhomogeneities is anomalously slow and the entanglement dynamics consistent with the logarithmic scaling in time expected in an MBL phase.

Numerical studies have provided evidence that strong interactions can stabilize inhomogeneous initial states resulting in a very slow thermalization process.<sup>30–33</sup> In Ref.23 the possibility was raised that strong interactions might even induce a delocalization-localization transition for such inhomogeneous initial states. Even more relevant for the following discussion are models consisting of a light and a heavy species which interact with each other.<sup>21,22,24,26</sup> Here the idea is that the heavy particles might create an effective disorder potential for the faster light particles driving potentially a transition where the light particles localize or, alternatively, leading to an extended regime in time where the light particles appear localized although the system becomes ultimately ergodic at very long times ('quasi MBL').

It is well known that both AL and MBL can occur in translationally invariant systems with two particle species if one of the species is static. Here the static particle species creates a discrete disorder potential for the mobile one.<sup>34</sup> In particular, the case of spinless fermions with a nearest-neighbor density-density interaction—which is equivalent to a  $s = 1/2$  XXZ spin chain by Jordan-Wigner transformation—in an effective

binary disorder potential has been studied in detail.<sup>10,11</sup>

In this paper we will extend these studies to the case where the second heavy species becomes mobile. Our goal is to study a specific microscopic model which does show an MBL phase in the static case and ask whether the MBL phase survives for small hopping amplitudes  $J'$  (in the sense of a diverging decay time for initial inhomogeneities) or at least shows a distinct time regime where MBL characteristics remain present. We will use an unbiased density-matrix renormalization group algorithm (see Sec. II for details) to obtain numerically exact results for the time evolution of the system after a quantum quench directly in the thermodynamic limit. We will concentrate on interactions between the two particle species which are effectively infinite in the time regime studied. The advantages of the numerical study presented here as compared to previous exact diagonalization and perturbative studies are that numerically exact results in the thermodynamic limit are obtained for a model which can be, in principle, realized in experiment.

Our paper is organized as follows. In Sec. II we introduce the considered  $s = 1/2$  spin ladder and discuss the numerical algorithm to calculate the dynamics of observables following the quench. We present results for the case where both legs of the spin  $s = 1/2$  ladder are of XX type in Sec. III. Results where the spins in one leg have an XXZ-type interaction are then discussed in Sec. IV. We summarize and conclude in Sec. V.

## II. MODEL AND METHODS

We start from a bosonic Hubbard model with two species  $a$  and  $b$  described by the Hamiltonian

$$\begin{aligned}
 H = & -\frac{J}{2} \sum_j (a_j^\dagger a_{j+1} + h.c.) - \frac{J'}{2} \sum_j (b_j^\dagger b_{j+1} + h.c.) \\
 & + \sum_j [V_a n_j^a n_{j+1}^a + U_a n_j^a (n_j^a - 1) + (a \leftrightarrow b)] \\
 & + D \sum_j n_j^a n_j^b. \quad (1)
 \end{aligned}$$

Here  $J$  and  $J'$  are hopping amplitudes and  $U_{a,b}$  the onsite repulsive interactions for the  $a, b$  particles respectively.  $D$  denotes the intraspecies interactions and we also include interspecies nearest-neighbor terms  $V_{a,b}$ .

We prepare the system of  $b$  particles in a Fock state  $|\Psi_b\rangle = \sum_{n_1^b, \dots, n_M^b} \alpha_{n_1^b, \dots, n_M^b} |n_1^b \dots n_M^b\rangle$  where  $n_j^b$  is the occupation number for the  $b$  particles at lattice site  $j$ .<sup>34</sup> The  $a$  particles, on the other hand, are prepared in an initial product state. If we now time evolve the system in the limit  $J' \rightarrow 0$  then the intraspecies interaction term turns into an effective discrete random potential for the mobile  $a$  particles with strengths  $D n_j^a n_j^b \rightarrow D P_j^b n_j^a$  where  $P_j^b \in \{0, 1, 2, \dots\}$  and the probability distribution is determined by  $|\alpha_{n_1^b, \dots, n_M^b}|^2$ . In the limit  $U_b \rightarrow \infty$  where

$n_j^b \in \{0, 1\}$ , in particular, a binary disorder potential is realized which has been shown to lead to many-body localization of the  $a$  particles at sufficiently large  $D$ .<sup>10,11</sup>

Here we are interested in investigating the case  $J' \neq 0$  with  $J' < J$ . The question then is if the heavy  $b$  particles can still serve as an effective dynamic binary disorder potential for the light  $a$  particles. In order to reduce the number of parameters in the model and to obtain numerical results for times much longer than  $1/J'$  we concentrate on the hardcore boson case  $U_{a,b} \rightarrow \infty$  with  $V_b = 0$ . In this limit the bosonic model (1) can be mapped onto the following spin model

$$\begin{aligned}
 H = & J \sum_j \left[ \frac{1}{2} (S_j^+ S_{j+1}^- + S_j^- S_{j+1}^+) + \Delta S_j^z S_{j+1}^z \right] \\
 & + J' \sum_j \frac{1}{2} (\sigma_j^+ \sigma_{j+1}^- + \sigma_j^- \sigma_{j+1}^+) + D \sum_j S_j^z \sigma_j^z \quad (2)
 \end{aligned}$$

with  $J\Delta = V_a$  and spin-1/2 operators  $S_j$  and  $\sigma_j$  representing the two species of hardcore bosons. For  $\Delta = 0$  this is *exactly the same model* which has been considered in Ref.26 for small clusters of up to  $L = 8$  sites.

Here we want to study this model in the *thermodynamic limit* for  $\Delta \in [0, 1]$ . As initial state for the spin ladder we consider  $|\Psi\rangle = |N\rangle_S \otimes |\infty\rangle_\sigma$  where  $|N\rangle = |\uparrow\downarrow\uparrow\downarrow \dots\rangle_S$  is the Néel state and  $|\infty\rangle_\sigma = \bigotimes_j \frac{1}{\sqrt{2}} (|+\rangle + |-\rangle)_j$  is the product state corresponding to an equal superposition of all arrangements of spins  $\sigma_j^z = +, -$ . Importantly, the time evolution starting from the product state  $|\infty\rangle_\sigma$  for  $J' = 0$  then gives an exact average over all possible effective binary magnetic field configurations,  $D\sigma_j^z \rightarrow h_j^{\text{eff}} = \pm D/2$ .<sup>10,11,34,35</sup> Note that for  $J' \neq 0$  this setup is no longer equivalent to averaging over the dynamics starting from each possible configuration for the slow particles separately. However, setting up the state  $|\infty\rangle_\sigma$  is in principle possible—for example in experiments on ultracold bosonic quantum gases described by the effective Hamiltonian (1)—and is an interesting starting point because it does include the case  $J' \rightarrow 0$  where an exact disorder average is obtained and a many-body localized phase is known to exist; see Ref.11 for a phase diagram of the model for  $J' = 0$  as a function of  $D$  and  $\Delta$ .

We want to stress that the dynamics at times  $t > 1/J'$  is not expected to be qualitatively different for different non-trivial initial states. In Appendix A we indeed show by exact diagonalizations that the dynamics starting from the chosen initial state is *qualitatively the same* as the dynamics obtained by averaging over initial product states as has been done in Ref.26.

We study the quench dynamics in the spin ladder (2) using the light cone renormalization group (LCRG) algorithm.<sup>10,11,33</sup> This algorithm makes use of the fact that even in the clean ergodic case, information and correlations for a generic Hamiltonian with short-range interactions only spread through the lattice at a *finite* (Lieb-Robinson) velocity  $v_{LR}$ .<sup>36</sup> Using a Trotter-Suzuki

decomposition for the time evolution operator the one-dimensional quantum model is first mapped onto a two-dimensional classical model. It then suffices to consider a finite light cone with Trotter velocity  $v_T \gg v_{LR}$  to be effectively in the thermodynamic limit. The light cone is extended and then truncated using a density-matrix renormalization group (DMRG) procedure propagating the initial state forward in time. The transfer matrices used to expand the light cone have dimension  $4\chi \times 4\chi$  for the spin ladder and we keep up to  $\chi = 20\,000$  states requiring up to 450 GB of RAM. We adapt the number of states  $\chi$  such that the truncation error is less than  $10^{-10}$  at small and intermediate times and at most  $10^{-7}$  at the longest simulation times shown.

We will concentrate here on two observables as a function of time  $t$  after the quench: the staggered magnetization  $m_s(t) = \sum_j (-1)^j \langle S_j^z \rangle$  and the entanglement entropy  $S_{\text{ent}}(t)$  when cutting the whole system—consisting of slow and fast particles—in two semi-infinite halves. The asymptotics of these two observables at long times allows to distinguish between different phases of the Hamiltonian (2): (i) If the system is in an AL phase then  $m_s(t \rightarrow \infty) \neq 0$  and  $S_{\text{ent}}(t \rightarrow \infty) \sim \text{const.}$  (ii) If the system is ergodic then  $m_s(t \rightarrow \infty) = 0$ . The entanglement entropy in the clean case without disorder grows linearly in time. (iii) Finally in the MBL phase,  $m_s(t \rightarrow \infty) \neq 0$  while asymptotically  $S_{\text{ent}} \sim \ln t$ .

In the following two sections we present our numerical results for the model (2) in the thermodynamic limit. The analysis of the scaling behavior is based on data for times  $t \lesssim 10/J'$ . The time scale  $t \sim D/J^2$  set by the intraparticle interaction  $D$ —which is very large in our simulations and effectively infinite in the time intervals studied—is out of reach and plays no role. The obtained scaling of  $m_s(t)$  and  $S_{\text{ent}}(t)$  is valid in the regime  $1/J < t < D/J^2$  while fully ergodic behavior is expected to set in at the longest time scale  $t > D/(J')^2$ .

### III. THE XX CASE

For  $\Delta = 0$  the interactions on both legs of the spin ladder (2) are of XX type. For  $J' = 0$  we can map the model by a Jordan-Wigner to non-interacting spinless fermions subject to a binary disorder potential of strength  $D$ . For  $D \neq 0$  we thus expect the model to be in an AL phase. Interestingly, the model becomes interacting by allowing for a finite hopping  $J'$ . I.e., we expect that the hopping drives a transition from an AL phase of non-interacting fermions to an interacting phase.

To investigate this transition, we concentrate on the case  $D \gg J > J' > 0$ . Then there is an energy cost  $D$  associated with flipping two neighboring spins  $\mathbf{S}_j$ ,  $|\uparrow\downarrow\rangle \rightarrow |\downarrow\uparrow\rangle$ , if the spins  $\sigma_j$  are antiparallel as well. One might therefore expect that second order processes are required for the heavy species to become mobile by either moving on their own with effective hopping amplitude  $J'_{\text{eff}} = (J')^2/D$  or by moving together with the lighter

species with effective hopping amplitude  $J_c = JJ'/D$ . This then would give rise to time scales  $t'_{\text{eff}} = 1/J'_{\text{eff}}$  and  $t_c = 1/J_c$  respectively. Note that these timescales are effectively infinite for the time intervals studied numerically in the following because we set  $D/J = 4000$ .

If these are the only relevant time scales, then the staggered magnetization  $m_s(t)$  will remain essentially constant for times  $t < \min(t'_{\text{eff}}, t_c)$  and we then might indeed expect a time regime where the system appears localized. In the following we will, however, show that this is not the case and that the dynamics is actually more complicated: neighboring clusters where spins  $\sigma_j$  are parallel can act as a 'bath' and a decay of  $m_s(t)$  already sets in at much smaller time scales.

Let us start with the simplest case of  $J' = 0$ . Then the chain effectively separates into finite segments with equal potentials  $\pm D$ .<sup>10</sup> The probability to find a segment of length  $\ell$  is given by  $p_\ell = \ell/2^{\ell+1}$  and the magnetization becomes

$$m_s(t \ll D/J^2) = \sum_\ell p_\ell m_s^\ell(t) \quad (3)$$

where  $m_s^\ell$  is the staggered magnetization for a segment of length  $\ell$ . At times  $1/J \ll t \ll D/J^2$  the staggered magnetization then oscillates around  $1/6$  and only the odd clusters contribute to the non-zero average.<sup>10</sup> For  $J' = 0$  there is thus no decay at times  $t \ll D/J^2$ . While this simple picture breaks down at times  $t > D/J^2$ ,  $m_s(t)$  will remain finite because any amount of potential disorder will lead to Anderson localization in one dimension.

Turning on a weak hopping for the heavy species we would expect that  $m_s(t)$  remains largely unchanged for times  $t < \min(t', t_c)$  if the discussed second order processes involving the large energy scale  $D$  are the only ones which can lead to a relaxation. This is, however, not the case as can clearly be seen from the unbiased numerical data shown in Fig. 1. Instead, the data are consistent with an exponential decay  $m_s(t) \sim \exp(-\gamma t)$  with a relaxation rate  $\gamma \sim A \cdot (J')^\beta$  with  $\beta = 1.89 \pm 0.1$  and an amplitude  $A \approx 1.2$  which is three orders of magnitude larger than expected if the responsible processes would involve the large energy scale  $D$  (see inset of Fig. 1). This suggests that there is another mechanism which leads to a relaxation of  $m_s(t)$ . This mechanism is depicted in Fig. 2. If we think of flips of neighboring spins as gates applied at a particular time step in a Trotter-Suzuki decomposition of the time evolution operator, then we see that three time steps are required to flip all the spins  $S_j^z$  for the single barrier case shown in Fig. 2. Similar processes also exist for larger barriers. We also note that this process *is generic and is important for the dynamics independent of the initial state*. If  $N$  is the number of consecutive  $' + -'$  configurations of  $\sigma_j^z$  (number of barriers) then we find that  $N + 2$  time steps are required to overcome the barrier. This implies a dephasing time  $\tau \sim f(J', D)N$  across such barriers where  $f(J', D)$  is a function depending on the hopping  $J'$  and the intraparticle interaction  $D$ . We want to stress once more that

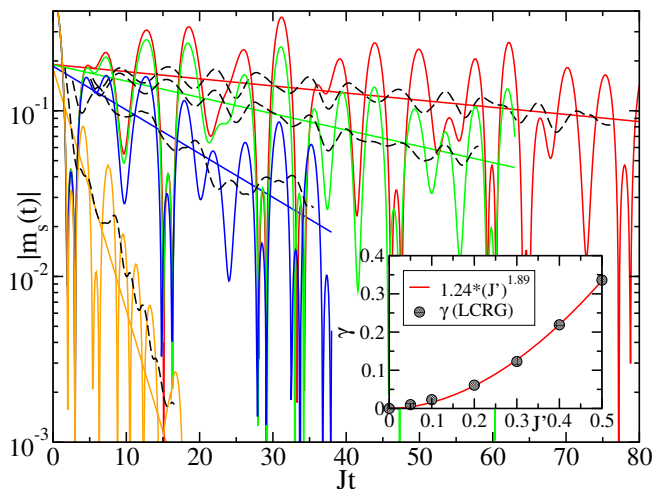


FIG. 1: Main: Staggered magnetization  $m_s(t)$  at  $\Delta = 0$  and  $D = 4000$ . Shown are LCRG results (solid curves), exponential fits (solid lines), and running averages (dashed lines, guide to the eye) for  $J' = 0.05, 0.1, 0.2, 0.5$  (from top to bottom). Inset: Relaxation rate  $\gamma$  extracted from the exponential fits as a function of hopping amplitude  $J'$  (symbols) and a power-law fit (solid curve).

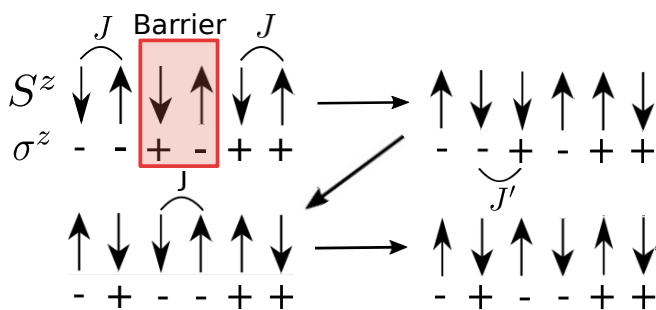


FIG. 2: From left to right, top to bottom: In the initial state the spins  $S_j^z$  (arrows) are in a Néel state, the spins  $\sigma_j^z$  (+/-) in an equal superposition of all configurations. A '+ -' arrangement creates a barrier for spin flips. A three-step process, however, allows to flip all the spins  $S_j^z$  without involving the large energy scale  $D$ .

we are concerned with the regime  $D \gg J > J'$  where the processes depicted in Fig. 2 set the relevant time scale for dephasing and not  $J'_{\text{eff}}$  and  $J_c$  which involve the numerically infinite energy scale  $D$ . In this case, the staggered magnetization at time  $t$  is dominated by clusters of size  $N \geq N_0 = f^{-1}(J', D)t$  which occur with probability  $P(N)$  and have remained static. This implies a scaling<sup>11</sup>

$$m_s(t) \sim \int_{N_0}^{\infty} P(N) dN \sim \int_{f^{-1}(J', D)t}^{\infty} \frac{dN}{2^{2N}} \sim e^{-\frac{t}{f(J', D)}}. \quad (4)$$

I.e., these considerations imply that *as soon as  $J' \neq 0$  there is a finite decay rate  $\gamma \sim f^{-1}(J', D)$ .*

It is also worth comparing this to the case of small quenched binary disorder where the system is close to

the MBL phase but still on the ergodic side. In this case the time to overcome barriers between thermalizing clusters scales as  $\tau \sim e^N$ . Using again Eq. (4) then leads to a much slower power-law decay of the staggered magnetization.<sup>11</sup> The system with mobile heavy particles is thus *qualitatively different* from a system with quenched disorder close to the ergodic-MBL phase transition.

If the spin inhomogeneity can decay, then we also expect that information can spread beyond the finite segments which form for  $J' = 0$ . We therefore investigate the entanglement entropies between the two halves of the infinite ladder next. The data shown in Fig. 3 are con-

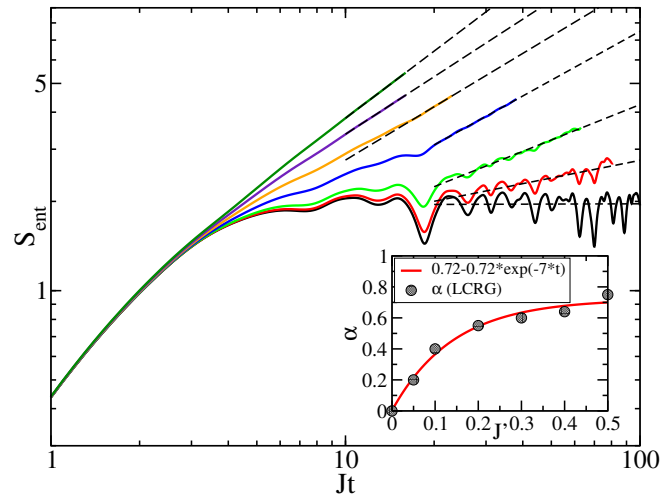


FIG. 3: Main: Entanglement entropy at  $\Delta = 0$  and  $D = 4000$ . Shown are LCRG results (solid curves) for  $J' = 0, 0.05, 0.1, 0.2, \dots, 0.5$  (bottom to top) and power-law fits (dashed lines). Inset: Power-law exponent  $\alpha$  as a function of hopping amplitude  $J'$ .

sistent with a power-law scaling,  $S_{\text{ent}}(t) \sim t^\alpha$ , with an exponent  $\alpha$  which changes monotonically as a function of the hopping amplitude  $J'$  (see inset of Fig. 3). For  $J' \sim J$  and  $D = 4000$  the exponent seems to saturate to a value  $S_{\text{ent}} \approx 1/\sqrt{2} \approx 0.71$ .

It is important to note that the process depicted in Fig. 2 is a process which allows for the dephasing of the staggered magnetization inside barriers. Thus  $\tau \sim N$  is a dephasing time. It is *not* the time required to transport information across a barrier of size  $N$ . If this would be the case then  $S_{\text{ent}} = vt$  and only the velocity  $v$  would change as a function of  $J'$ . That the dephasing time  $\tau$  and the entanglement time  $\tau_{\text{ent}}$  are different can be understood already in a classical picture: Imagine e.g. the left spin in the initial configuration shown in Fig. 2 as being distinguishable from the other down spins. Trying to move this spin from the left to the right end of the segment across the barrier, it becomes obvious that many more time steps are required than for simply flipping all spins of the segment. Thus we expect  $\tau_{\text{ent}} \gg \tau$  as well as a different scaling with the size of the barrier.

The entanglement entropy is proportional to the entangled region. Thus if  $\tau_{\text{ent}} \sim e^N$  then  $S_{\text{ent}} \sim \ln t$  as in the MBL phase. If, on the other hand,  $\tau_{\text{ent}} \sim N^{1/\alpha}$  with  $\alpha < 1$  then this leads to the observed sub-ballistic increase,  $S_{\text{ent}} \sim t^\alpha$ . Because of the very strong coupling  $D = 4000$  between the legs, information spreading is sub-ballistic for  $t < D/J^2$  even if  $J' \sim J$ . We expect that this sub-ballistic behavior will give way to a ballistic spreading at times  $t > \min(t'_{\text{eff}}, t_c) > D/J^2$ . Studying the latter regime is outside the scope of this article.

One of the main observations in Ref.26, where the model (2) was studied for  $\Delta = 0$  on small clusters of up to  $L = 8$  sites, was that in the dynamics distinct time scales are visible, in particular, in the time evolution of the entanglement entropy. More precisely, the study identified the time scales  $1/J$ ,  $1/J'$ ,  $e^L/J'$ , and  $D/(J')^2$ . The latter two time scales are irrelevant in our study because we are in the thermodynamic limit and restrict ourselves to effectively infinite  $D$ . In the remaining regimes the authors identified the following behavior for  $S_{\text{ent}}(t)$ : (i)  $0 < t < 1/J$ : initial growth, (ii)  $1/J < t < 1/J'$ : single-particle localized plateau, and (iii)  $t > 1/J'$ : a logarithmic growth. In App. A we show that the same time regimes are also visible for the initial state chosen in our study if we consider the same  $L = 8$  cluster. The differences between Ref.26 and our LCRG results are *not* a result of different initial conditions but rather of the different regimes investigated ( $L \ll t$  versus the thermodynamic limit). In particular, in the thermodynamic limit results for  $m_s(t)$  in Fig. 1 and  $S_{\text{ent}}(t)$  in Fig. 3 no qualitative changes occur at the time scale  $1/J'$ . Instead  $m_s(t)$  shows an exponential decay for all times  $Jt \gtrsim 5$  while the asymptotic power-law scaling for  $S_{\text{ent}}(t)$  sets in for  $Jt \gtrsim 20$  independent of  $J'$ . What does change as a function of  $J'$  in a smooth way are the decay rate  $\gamma$  and the power-law exponent  $\alpha$  with *both*  $\gamma, \alpha \rightarrow 0$  for  $J' \rightarrow 0$ . To confirm this picture we have also calculated both quantities for small  $J'$  such that  $1/J' \in [20, 1000]$ . The results are shown in Fig. 4 and are fully consistent with an onset of scaling independent of  $J'$ . To summarize, we have obtained a picture which is very different from the one described in Ref.26 for small clusters: There is no single-particle localized plateau in  $S_{\text{ent}}(t)$  for  $1/J < t < 1/J'$  in the thermodynamic limit. In fact, the scale  $1/J'$  is not visible at all in our data. There is also no quasi MBL regime for  $1/J' < t \ll D/(J')^2$  with logarithmic entanglement growth. Instead, we find a scaling regime which becomes established at  $Jt \gtrsim 20$  independent of  $J'$  in which  $m_s(t) \sim e^{-\gamma t}$  and  $S_{\text{ent}}(t) \sim t^\alpha$  with  $\alpha < 1$  where both  $\gamma, \alpha$  are smooth functions of  $J'$ . We have argued that this behavior can be explained by barriers of size  $N$  and a related dephasing time which scales as  $\tau \sim N$  while the entanglement time across a barrier scales as  $\tau_{\text{ent}} \sim N^{1/\alpha}$ . Thus we have identified a time regime with sub-ballistic entanglement spreading different *both* from normal ergodic as well as MBL behavior. The exact diagonalization results presented in App. A clearly demonstrate that the behavior found in Ref.26 is

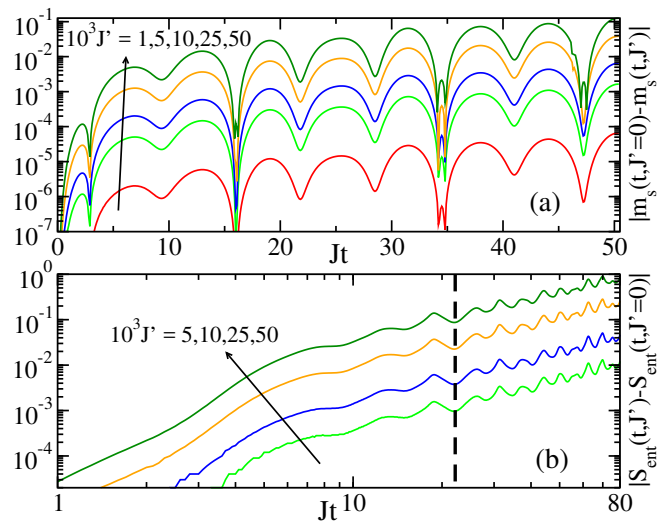


FIG. 4: (a) Difference between  $m_s(t)$  for finite  $J'$  and  $m_s(t)$  for  $J' = 0$ . After a rapid increase an exponential decay sets in for  $Jt \gtrsim 5$ . (b) Difference between  $S_{\text{ent}}(t)$  for zero and finite  $J'$ . A power-law scaling with a small exponent  $\alpha$  sets in for  $Jt \gtrsim 20$  (dashed line). In both cases the onset of scaling is independent of  $J'$ .

the result of finite-size effects and does not describe the behavior in the thermodynamic limit. Given that there is no quenched disorder, this should not come as a complete surprise.

#### IV. THE XXZ CASE

Next, we study the case where the spins  $\mathcal{S}_j$  are interacting,  $0 < \Delta \leq 1$  to obtain additional evidence for the mechanism depicted in Fig 2. For  $J' = 0$  and  $D \gtrsim 0.3$  the system is then in an MBL phase where  $m_s(t)$  does not decay and  $S_{\text{ent}} \sim \ln t$ .<sup>11</sup> Turning on the hopping  $J'$  is expected to drive a phase transition from the MBL into an ergodic phase.

##### A. Weak and intermediate interactions

We start by analyzing the numerical data for  $m_s(t)$  as a function of  $J'$  for  $\Delta = 0.2$  and  $\Delta = 0.6$ , see Fig. 5. While the oscillations in the magnetization curves are damped as compared to the  $\Delta = 0$  case shown in Fig. 1, they still show an exponential decay for  $Jt \gtrsim 5$ . The relaxation rate  $\gamma$  extracted from the fits increases monotonically with  $J'$  with the exponent of the power-law scaling,  $\gamma = A(J')^\beta$ , decreasing with increasing  $\Delta$ . We notice, furthermore, that while the amplitude  $A$  is similar to the XX case for  $\Delta = 0.2$ , it is an order of magnitude smaller for  $\Delta = 0.6$ : At intermediate interaction strengths we observe a pronounced slowing down of the relaxation (see also Fig. 9).

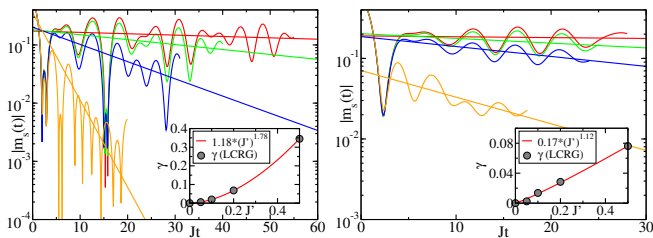


FIG. 5:  $m_s(t)$  for  $\Delta = 0.2$  (left) and  $\Delta = 0.6$  (right). Curves are LCRG data and lines exponential fits as function of hopping  $J'$ . Insets: Decay rates  $\gamma$  as function of hopping  $J'$ .

The entanglement entropy, shown in Fig. 6, also shows a behavior very similar to the  $\Delta = 0$  case. The only qualitative difference is the logarithmic scaling for  $J' = 0$  indicative of the MBL phase. The fitted exponents  $\alpha$  of a

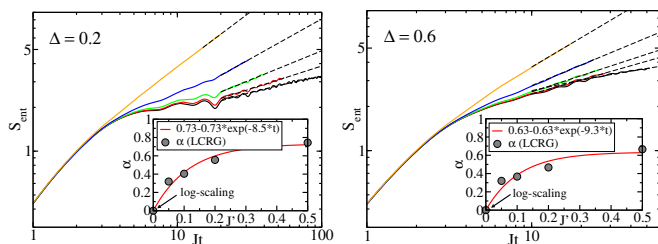


FIG. 6: Entanglement entropies for  $\Delta = 0.2$  and  $\Delta = 0.6$  and  $J' = 0, 0.05, 0.1, 0.2, 0.5$  (from bottom to top). The behavior is qualitatively similar to the  $\Delta = 0$  case shown in Fig. 3 except for  $J' = 0$  where  $S_{\text{ent}} \sim \ln t$ .

power-law scaling (see inset of Fig. 6) are again consistent with a sub-ballistic power-law scaling  $S_{\text{ent}}(t) \sim t^\alpha$  with  $\alpha \approx 0.73$  for large  $J'$ .

In summary, interactions  $\Delta$  reduce the relaxation rate  $\gamma$ . The initial Néel state decays slower. Considering the dephasing process shown in Fig. 2 this is not surprising. The flips of the spins  $\mathbf{S}_j$ —required to make the barrier formed by the spins  $\boldsymbol{\sigma}_j$  mobile—lead to a local ferromagnetic arrangement. For finite  $\Delta$  this now involves an energy cost. The numerical results nevertheless show that the dephasing time across the barrier has the same functional form given by  $\tau = f(J', D, \Delta)N$  with a function  $f(J', D, \Delta)$  which is growing with increasing  $\Delta$ . The sub-ballistic scaling of the entanglement entropy is qualitatively not affected by the interaction.

## B. The Heisenberg case

Finally, we also want to investigate the case of an  $SU(2)$  symmetric exchange on one of the legs, i.e. the case  $\Delta = 1$  in Eq. (2). For the staggered magnetization we still find an exponential decay for small  $J'$ , however, the relaxation rate is now extremely small (see Fig. 7). Furthermore, the data for  $J' = 0.7$  show large irregular oscillations and no clear scaling. A likely explanation is that the numerically

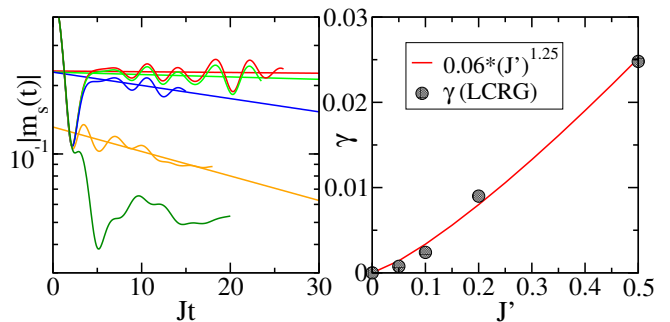


FIG. 7:  $m_s(t)$  for  $\Delta = 1.0$  and  $J' = 0.05, 0.1, 0.2, 0.5, 0.7$  (left panel, from top to bottom). The data are consistent with a very slow exponential decay with relaxation rates  $\gamma$  (right panel) except for  $J' = 0.7$  where in the accessible time range no clear scaling is observed.

accessible time scales are just too limited in this case. For the couplings  $J' \in [0, 0.5]$ , on the other hand, the relaxation rate again shows a power-law scaling with a similar exponent as for  $\Delta = 0.6$  but with an amplitude which is reduced by another factor of 3. This is consistent with the process depicted in Fig. 2.

The entanglement entropy changes very little as compared to the  $\Delta = 0.6$  case (see Fig. 8). Power-law fits

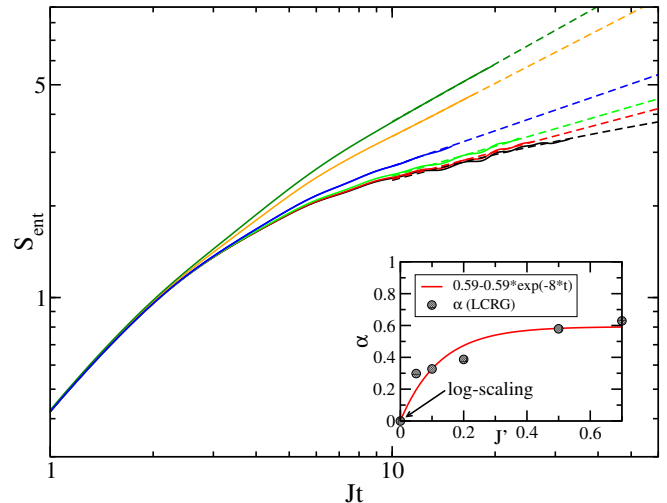


FIG. 8: Entanglement entropy for  $\Delta = 1.0$  and  $J' = 0, 0.05, 0.1, 0.2, 0.5, 0.7$  (from bottom to top). Inset: Exponent  $\alpha$  as a function of  $J'$ .

still describe the data well for  $Jt \gtrsim 10$ . The onset of the power-law scaling remains independent of  $J'$ . For the extracted exponent  $\alpha$  the behavior as function of  $J'$  is still the same as for the smaller  $\Delta$  values, although the data are a bit more scattered around the fit function. This is likely a consequence of the limited times accessible numerically for  $\Delta = 1$ : The fits are more affected by oscillations on short time scales and thus less reliable. Finally, we want to remark that there is no extended regime in time where the entanglement growth

is independent of  $J'$ . This is contrary to the results for small clusters discussed in Ref.26 showing again that the results for such small system sizes are not indicative of the behavior in the thermodynamic limit but are rather dominated by finite size effects.

## V. CONCLUSIONS

We have investigated quench dynamics in a spin ladder with a large coupling  $\sim DS_j^z \sigma_j^z$  along the rungs which is effectively infinite in the time regime investigated. While the spins  $\mathbf{S}_j$  with exchange amplitude  $J$  and interaction  $\Delta$  were prepared in a Néel state, the spins in the other leg with exchange amplitude  $J'$  were prepared in a product state  $\bigotimes_j (|+\rangle + |-\rangle)_j / \sqrt{2}$ . For  $J' = 0$  the spins  $\sigma_j$  realize a quenched binary disorder potential for the spins  $\mathbf{S}_j$ . In this case, the model is either in an AL phase ( $\Delta = 0$ ) or an MBL phase ( $\Delta \neq 0$ ).

Using an infinite-size density-matrix renormalization group algorithm we have addressed the question whether the MBL phase can survive for finite  $J'$  ('MBL without disorder') or if there is an extended regime in time where the model for finite  $J'$  still shows the characteristics of the MBL phase ('quasi MBL') including a logarithmic increase of the entanglement entropy and memory of the initial state. To answer these questions we have investigated the Néel order parameter  $m_s(t)$  and the entanglement entropy  $S_{\text{ent}}(t)$  between two semi-infinite halves of the ladder as a function of time  $t$  after the quench. The results clearly show that there is no MBL phase for finite  $J'$  and also no time regime where MBL characteristics persist. The time regime  $1/J < t \ll D/J^2$  for  $J' \neq 0$  is instead characterized by an exponential polarization decay  $m_s(t) \sim e^{-\gamma t}$  with decay rate  $\gamma = \gamma(J', D, \Delta)$  while the entanglement entropy grows sub-ballistically,  $S_{\text{ent}}(t) \sim t^\alpha$  with  $\alpha < 1$ . The latter behavior is "in between" the logarithmic growth in the MBL phase and the linear growth expected when the system becomes fully ergodic.

An analysis of the numerical results for the decay rate of the staggered magnetization for different  $J'$  and  $\Delta$  is consistent with

$$\gamma \propto e^{-\Delta} J'^\beta \quad (5)$$

where  $\beta \in [1, 2]$  is a weakly  $\Delta$ -dependent exponent while the amplitude of the power-law scaling is exponentially suppressed with increasing  $\Delta$ , see Fig. 9. These results—including the exponential suppression of the amplitude with increasing  $\Delta$ —is consistent with the mechanism for the staggered magnetization decay explained and depicted in Fig. 2.

Our results are quite different from those obtained in a previous exact diagonalization study, Ref.26, which concentrated mostly on the  $\Delta = 0$  case. In the latter study distinct time regimes including a quasi MBL phase in time were identified. None of this is confirmed in our

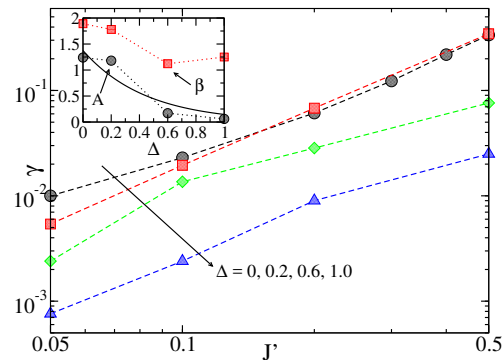


FIG. 9: Relaxation rates  $\gamma$  extracted from the decay of  $m_s(t)$  as a function of  $J'$  for various  $\Delta$ . The results are consistent—with some larger deviations for  $\Delta = 0.6$ —with a power-law scaling. Inset: Parameters  $A, \beta$  obtained from fits  $\gamma = A(J')^\beta$ . The amplitude  $A$  is well fitted by  $A(\Delta) = 1.4 \cdot \exp(-2.2\Delta)$  (solid line).

study for infinite-size systems. The comparison with exact diagonalization data presented in App. A clearly show that the plateaus in  $S_{\text{ent}}(t)$  are a consequence of finite-size effects and are not present in the thermodynamic limit.

In conclusion, we studied a prototypical model which has been put forward as showing MBL without disorder or quasi MBL behavior and concluded that neither one is realized. Our study, however, does not exclude that different models exist which do show quasi MBL regimes or where a power-law scaling of the entropy with a small exponent is difficult to distinguish from a logarithmic growth.<sup>27</sup>

## Acknowledgments

The author thanks T. Enns for discussions at an early stage of the project. We acknowledge support by the Natural Sciences and Engineering Research Council (NSERC, Canada) and by the Deutsche Forschungsgemeinschaft (DFG) via Research Unit FOR 2316. We are grateful for the computing resources provided by Compute Canada and Westgrid as well as for the GPU unit made available by NVIDIA.

## Appendix A: Exact diagonalization results

The model (2) for  $\Delta = 0$  is exactly the same model which has been studied in Ref.26 by exact diagonalizations of ladders of up to  $L = 8$  sites. A difference between the previous study and the results presented here for infinite systems size are the initial states. While in the former case results for averages over 30–100 initial product states were presented with the constraint that the same number of up and down spins are present on each leg, we

have considered a single initial state in which the spins on one leg were prepared in the Néel state and the spins on the other leg in the state  $|\infty\rangle_\sigma = \bigotimes_j \frac{1}{\sqrt{2}}(|+\rangle + |-\rangle)_j$ . Given that the system does not contain quenched disorder, the precise initial state—as long as it is non-trivial—should not *qualitatively* affect the dynamics at times  $t > 1/J'$ . This is supported by exact diagonalization data for ladders with  $L = 8$  sites ( $N = 16$  total lattice sites) shown in Fig. 10. Here the dynamics obtained by taking averages over initial product states as in Ref.26 is compared with dynamics starting from the initial state  $|\Psi\rangle = |N\rangle_S \otimes |\infty\rangle_\sigma$  as used in this study.

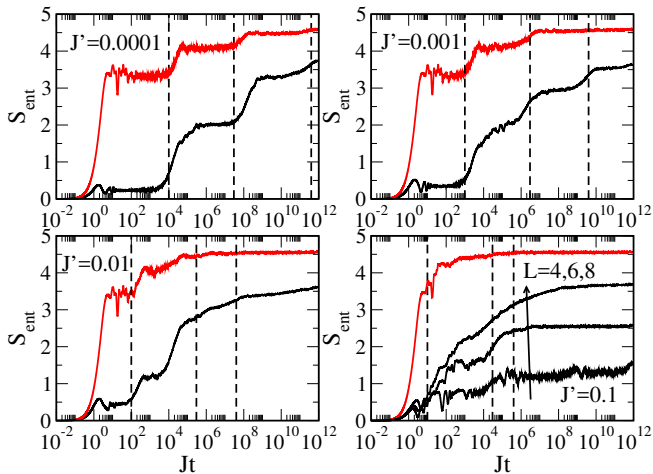


FIG. 10: Entanglement entropy during time evolution with the Hamiltonian (2) for  $D = 4000$  and  $\Delta = 0$  and different  $J'$  for a  $L = 8$  ladder. The black lines are results for an average over 100 initial product states, the red lines the result for the initial state  $|\Psi\rangle = |N\rangle_S \otimes |\infty\rangle_\sigma$ . Dashed vertical lines denote the energy scales  $1/J'$ ,  $e^L/J'$ ,  $D/(J')^2$  (from left to right). For  $J' = 0.1$ , data for  $L = 4, 6$  are shown in addition. The time step in the numerical data is  $\log_{10}(t_{n+1}/t_n) = 0.001$  and running averages over 100 time steps are shown for clarity.

Importantly, the results for small  $J'$  are qualitatively the same for both sets of initial states. An initial rapid increase up to time  $\sim 1/J$  is followed by a first plateau which stretches out to  $\sim 1/J'$ . The entanglement entropy then increases again and reaches another plateau which lasts up to the finite size scale  $\sim e^L/J'$ . This is followed by another increase and another plateau extending up to the scale  $D/(J')^2$ . Our exact diagonalization results thus confirm the results found in Ref.26 for small clusters.

For larger  $J'$  these structures are somewhat less visible, in particular, if we start in the initial state  $|\Psi\rangle = |N\rangle_S \otimes |\infty\rangle_\sigma$  because the entanglement is larger and is limited by the maximally possible entanglement for this cluster size ( $S_{\text{ent}}^{\text{max}} = 8 \ln 2 \approx 5.5$ ).

From the data for different system sizes obtained by averaging over initial product states with  $J' = 0.1$  shown in the lower right panel of Fig. 10 it becomes clear that the plateaus in the entanglement entropy are the result of the finite-size structure of the spectrum: For a total number of sites of the ladder  $N = 2L > 1/J'$  they completely disappear.

Finally, we want to demonstrate that the exact diagonalization data cannot be used to infer the behavior of the system in the thermodynamic limit after the first rapid increase of  $S_{\text{ent}}(t)$ , i.e. for times  $t > 1/J$ . The direct comparison of the LCRG data in the thermodynamic limit with exact diagonalization data for the initial state  $|\Psi\rangle = |N\rangle_S \otimes |\infty\rangle_\sigma$  presented in Fig. 11 makes it clear that the generic power-law increase of the entanglement entropy for times  $t \gtrsim 1/J$  and  $J' \neq 0$  is missed in exact diagonalizations which instead show a plateau because of finite size effects.

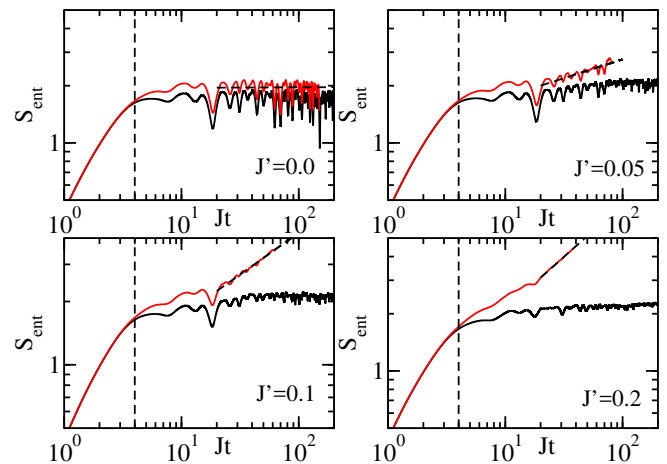


FIG. 11:  $S_{\text{ent}}(t)$  during time evolution with the Hamiltonian (2) starting from the initial state  $|\Psi\rangle = |N\rangle_S \otimes |\infty\rangle_\sigma$  for  $D = 4000$ ,  $\Delta = 0$  and different  $J'$ . Compared are exact diagonalizations for  $L = 8$  ladders (black lines) with LCRG data in the thermodynamic limit (red lines with dashed lines representing power-law fits). Both only agree for  $t \lesssim 1/J$  (dashed vertical line) due to finite size effects.

<sup>1</sup> P. W. Anderson, Phys. Rev. **109**, 1492 (1958).

<sup>2</sup> E. Abrahams, P. W. Anderson, D. C. Licciardello, and T. V. Ramakrishnan, Phys. Rev. Lett. **42**, 673 (1979).

<sup>3</sup> E. Abrahams, ed., *50 Years of Anderson Localization* (World Scientific, 2010).

<sup>4</sup> G. Roati, C. D'Errico, L. Fallani, M. Fattori, C. Fort,

M. Zaccanti, G. Modugno, M. Modugno, and M. Inguscio, Nature **453**, 895 (2008).

<sup>5</sup> J. Billy, V. Josse, Z. Zuo, A. Bernard, B. Hambrecht, P. Lugan, D. Clément, L. Sanchez-Palencia, P. Bouyer, and A. Aspect, Nature **453**, 891 (2008).

<sup>6</sup> H. Hu, A. Strybulevych, J. H. Page, S. E. Skipetrov, and

- B. A. van Tiggelen, *Nat. Phys.* **4**, 945 (2008).
- <sup>7</sup> D. Basko, I. Aleiner, and B. Altshuler, *Ann. Phys.* **321**, 1126 (2006).
- <sup>8</sup> A. Pal and D. A. Huse, *Phys. Rev. B* **82**, 174411 (2010).
- <sup>9</sup> J. Z. Imbrie, *Phys. Rev. Lett.* **117**, 027201 (2016).
- <sup>10</sup> F. Andraschko, T. Enss, and J. Sirker, *Phys. Rev. Lett.* **113**, 217201 (2014).
- <sup>11</sup> T. Enss, F. Andraschko, and J. Sirker, *Phys. Rev. B* **95**, 045121 (2017).
- <sup>12</sup> D. J. Luitz, N. Laflorencie, and F. Alet, *Phys. Rev. B* **91**, 081103 (2015).
- <sup>13</sup> D. J. Luitz, N. Laflorencie, and F. Alet, *Phys. Rev. B* **93**, 060201 (2016).
- <sup>14</sup> R. Vosk, D. A. Huse, and E. Altman, *Phys. Rev. X* **5**, 031032 (2015).
- <sup>15</sup> A. C. Potter, R. Vasseur, and S. A. Parameswaran, *Phys. Rev. X* **5**, 031033 (2015).
- <sup>16</sup> R. Nandkishore and D. A. Huse, *Annual Review of Condensed Matter Physics* **6**, 15 (2015).
- <sup>17</sup> E. Altman and R. Vosk, *Annual Review of Condensed Matter Physics* **6**, 383 (2015).
- <sup>18</sup> M. Žnidarič, T. Prosen, and P. Prelovšek, *Phys. Rev. B* **77**, 064426 (2008).
- <sup>19</sup> J. H. Bardarson, F. Pollmann, and J. E. Moore, *Phys. Rev. Lett.* **109**, 017202 (2012).
- <sup>20</sup> M. Schreiber, S. S. Hodgman, P. Bordia, H. P. Lüschen, M. H. Fischer, R. Vosk, E. Altman, U. Schneider, and I. Bloch, *Science* **349**, 842 (2015).
- <sup>21</sup> M. Schiulaz and M. Müller, *AIP Conf. Proc.* **1610**, 11 (2014).
- <sup>22</sup> M. Schiulaz, A. Silva, and M. Müller, *Phys. Rev. B* **91**, 184202 (2015).
- <sup>23</sup> G. Carleo, F. Becca, M. Schir?, and M. Fabrizio, *Sci. Rep.* **2**, 243 (2012).
- <sup>24</sup> T. Grover and M. P. A. Fisher, *J. Stat. Mech.* p. P10010 (2014).
- <sup>25</sup> W. De Roeck and F. Huveneers, *Phys. Rev. B* **90**, 165137 (2014).
- <sup>26</sup> N. Y. Yao, C. R. Laumann, J. I. Cirac, M. D. Lukin, and J. E. Moore, *Phys. Rev. Lett.* **117**, 240601 (2016).
- <sup>27</sup> A. A. Michailidis, M. Žnidarič, M. Medvedyeva, D. A. Abanin, T. c. v. Prosen, and Z. Papić, *Phys. Rev. B* **97**, 104307 (2018).
- <sup>28</sup> Y. Bar Lev, G. Cohen, and D. R. Reichman, *Phys. Rev. Lett.* **114**, 100601 (2015).
- <sup>29</sup> K. Kudo and T. Deguchi, *arXiv: 1803.06474* (2018).
- <sup>30</sup> C. Kollath, A. M. Läuchli, and E. Altman, *Phys. Rev. Lett.* **98**, 180601 (2007).
- <sup>31</sup> P. Barmettler, M. Punk, V. Gritsev, E. Demler, and E. Altman, *Phys. Rev. Lett.* **102**, 130603 (2009).
- <sup>32</sup> P. Barmettler, M. Punk, V. Gritsev, E. Demler, and E. Altman, *New J. Phys.* **12**, 055017 (2010).
- <sup>33</sup> T. Enss and J. Sirker, *New J. Phys.* **14**, 023008 (2012).
- <sup>34</sup> B. Paredes, F. Verstraete, and J. I. Cirac, *Phys. Rev. Lett.* **95**, 140501 (2005).
- <sup>35</sup> B. Tang, D. Iyer, and M. Rigol, *Phys. Rev. B* **91**, 161109 (2015).
- <sup>36</sup> E. H. Lieb and D. W. Robinson, *Commun. Math. Phys.* **28**, 251 (1972).